

Electrocatalytic Performance of PtSn/C-In₂O₃.SnO₂ Nanoparticles Prepared by Sodium Borohydride Reduction Process for Ethanol Oxidation in Acidic and Alkaline Electrolytes

C.V. Pereira¹, E.H. Fontes¹, J. Nandenha¹, M.H.M.T. Assumpção² and A.O. Neto^{1,*}

¹ Instituto de Pesquisas Energéticas e Nucleares, IPEN/CNEN-SP, Av. Prof. Lineu Prestes, 2242 Cidade Universitária, CEP 05508-000, São Paulo, SP, Brazil

² Universidade Federal de São Carlos, UFSCar Campus Lagoa do Sino, Rodovia Lauri Simões de Barros Km 12, CEP 18290-000 – Buri – São Paulo, SP (Brazil)

*E-mail: aolivei@ipen.br

Received: 23 June 2018 / Accepted: 20 August 2018 / Published: 1 October 2018

PtSn/C-In₂O₃.SnO₂ electrocatalysts were prepared by the borohydride reduction method in the single step using H₂PtCl₆.6H₂O and SnCl₂.2H₂O as metal sources, sodium borohydride as reducing agent and a physical mixture of 85% Vulcan Carbon XC72 and 15% In₂O₃.SnO₂ (indium tin oxide – ITO) as support. PtSn/C-In₂O₃.SnO₂ electrocatalysts were characterized by X-ray diffraction (XRD), energy dispersive analysis (EDX), transmission electron microscopy (TEM), cyclic voltammetry (CV), chronoamperometry (CA) and polarization curves in alkaline and acidic electrolytes (single cell experiments). The diffractograms of PtSn/C-In₂O₃.SnO₂ electrocatalysts showed peaks associated to the face-centered cubic (fcc) structure of platinum, peaks which could be identified as a cassiterite SnO₂ phase or with Indium-doped SnO₂ (ITO) used as supports. TEM micrographs showed metal nanoparticles with average nanoparticle size between 2.4 and 2.7 nm. Ethanol oxidation in acidic and alkaline electrolytes was investigated at room temperature, by chronoamperometry (CA), where PtSn/C-In₂O₃.SnO₂ (70:30) showed the highest activity among all electrocatalysts in study considering ethanol oxidation for acid electrolyte, while for alkaline electrolyte the highest activity was observed for PtSn/C-In₂O₃.SnO₂ (50:50). Polarization curves at 100°C showed PtSn/C-In₂O₃.SnO₂ (70:30) with superior performance for ethanol oxidation for acidic electrolyte and PtSn/C (70:30) for alkaline electrolyte, when compared to Pt/C for both electrolytes. The best performance obtained by PtSn/C-In₂O₃.SnO₂ (70:30) in real conditions could be associated with the occurrence simultaneously of the bifunctional mechanism and electronic effect resulting from the presence of PtSn alloy or a synergetic effect between PtSn and In₂O₃.

Keywords: Borohydride reduction process, PtSn/C-In₂O₃.SnO₂, ethanol oxidation, acidic and alkaline electrolytes, polarization curves

1. INTRODUCTION

Nowadays, one of the most common ways of generating power is by burning fossil fuels, which has had a high impact on the environment [1]. Today, it is necessary an alternative power sources in order to mitigate the environmental damage caused by burning fossil fuels and to meet the growing demand for energy in our planet [1]. Consequently fuel cells have been considered as one of the most promising sources for application in portable, vehicles and stationary devices [2].

In the development of low temperature fuel cells it has been proposed the use of organic molecules such as methanol, ethanol and formic acid, however the use of ethanol has been considered a promising system for energy conversion in Brazil, due to the easy handling and transportation and the ability to exploit the already available fuel infrastructures [3]. However the main obstacle to using ethanol, it is the slow electro-oxidation reaction kinetics and the complete oxidation of ethanol to CO_2 . This is difficult due to the energy needed for breaking the C–C bond resulting in intermediates products that block active sites on the electrocatalyst surface fuel cells [4-6].

Platinum (Pt) is often used as an electrocatalyst for ethanol oxidation, however this metal has some disadvantages, because it can be contaminated by species derived from dissociation of organic molecules, therefore its oxidation is slow at low temperatures, lastly the platinum is a limited resource and costly, therefore it is important to develop more efficient electrocatalysts to use ethanol in direct ethanol (DEFC) [7-8].

Baranova et al [9] have reported that Pt was more active for ethanol oxidation in alkaline electrolyte in comparison with acidic electrolyte. For alkaline electrolyte was observed the formation of acetate and aldehyde rather than of CO_2 and water as full oxidation products, so these authors concluded that is necessary to add a second electrocatalyst component to Pt, such as Sn or Ru to improve oxidation. PtSn-based electrocatalysts had been shown good results for ethanol electro-oxidation in acidic electrolyte. The increase in the activity of these electrocatalysts was explained by the formation of acetic acid. However the complete ethanol electro-oxidation to CO_2 in a DEFC continues to be a great challenge [10].

One way, to improve the ethanol oxidation is by decorating, Pt electrocatalysts with some oxide such as In_2O_3 . This oxide has showed corrosion resistance, smaller decrease in the electrochemical active surface area in comparison with the carbon support, the best catalytic performance for the steam reforming of methanol, dehydrogenation of ethanol and also showed an improvement on the catalytic activity and stability for the electro-oxidation of ethanol [11-12].

Another way to improve ethanol oxidation is by improving the interaction between the support and the Pt what could be done by modifying the carbon support surface in order to form suitable functional groups and better chemical links at the Pt/C interface. It is also important to highlight that the durability strongly depends on the support since the support determines the dispersion and stabilization of the nanoparticles. Thus, the use of alternative supports have been increasing and among them SnO_2 has gain interest among researchers [13-14].

Henrique et al. [11] showed that a Pt/C- In_2O_3 . SnO_2 had superior performance for ethanol electro-oxidation in comparison with Pt/C in all potential range of interest for fuel cells (0.05-0.9V). The experiments at 100°C on direct ethanol fuel cells showed that the power density for the

Pt/C-In₂O₃.SnO₂ was 400% higher than the one obtained using Pt/C indicating an improved tolerance to intermediate adsorbed. The data from Fourier transform infrared spectroscopy showed that the addition of C-In₂O₃.SnO₂ to Pt favors a more complete oxidation of the ethanol molecule or oxidize ethanol directly to acetic acid in acidic electrolyte.

In this context, the aim of this work was to prepare PtSn/C-In₂O₃.SnO₂ electrocatalysts for the first time by sodium borohydride reduction process, in different Pt:Sn atomic ratios for ethanol oxidation in acidic and alkaline electrolytes. It is important to note that this work include electrochemical experiments and also single-ethanol fuel cell.

2. EXPERIMENTAL

PtSn/C-In₂O₃.SnO₂ electrocatalysts with different Pt:Sn atomic ratios were prepared by borohydride reduction process with 20 wt% of metal loading. These electrocatalysts were prepared using H₂PtCl₆.6H₂O (chloroplatinic acid - Aldrich) and SnCl₂.2H₂O (Aldrich) as metal sources, sodium borohydride (NaBH₄, Aldrich) as reducing agent and a physical mixture of 85% Vulcan Carbon XC72 and 15% ITO (In₂O₃.SnO₂ nanopowder < 50nm particle size, 85-90 wt% and 10-15 wt% SnO₂ Aldrich) as support. In this work was chosen a 85% Vulcan Carbon XC72 and 15% ITO as support based on Henrique et al. [11] works.

In the borohydride reduction process, firstly it was prepared a solution containing metal ions of Pt and Sn, water/2-propanol (50/50, v/v) and 85% Vulcan Carbon XC72 and 15% ITO. After the solution was submitted to an ultrasonic bath and a NaBH₄ solution in 0.01 mol L⁻¹ NaOH was added in one step under stirring at room temperature, then the resulting solution was maintained under stirring for an additional 30 minutes. Finally, the material was filtered, washed with ultrapure water and dried at 70°C for 2 hours.

In this work we also prepared Pt/C, Pt/C-In₂O₃.SnO₂ and PtSn/C (70:30) electrocatalysts as reference for studies on ethanol oxidation. The activity these electrocatalysts were compared with PtSn/C-In₂O₃.SnO₂ electrocatalysts prepared with different Pt:Sn atomic ratios. PtSn/C (70:30) was chosen, because of Colmati works [15], where it was showed that the activity for ethanol oxidation in linear sweep voltammetry experiments at room temperature is greatly enhanced, mainly at low potentials on Pt-Sn 3:1 electrocatalysts prepared by the formic acid method, however at the higher temperatures of the fuel cell, these reactions are favored for an increase of the Sn content in the alloyed state.

PtSn/C-In₂O₃.SnO₂ electrocatalysts with different Pt:Sn atomic were characterized by X-ray diffraction using a Rigaku diffractometer, model Miniflex II, with CuK α radiation source ($\lambda = 0.15406$ nm); the diffractograms were recorded in the range of $2\theta = 20$ to 90° , with a step size of 0.05° and a scan time of 2 seconds per step, while the morphology, distribution, and the size of the nanoparticles were determined in a JEOL electron microscope model JEM-2100 operated at 200 kV by measuring 150 nanoparticles from 10 micrographs. A microscope Phillips XL30 working at 20 kV and equipped with EDAX DX4 microanalyzer was utilized for to obtain the Pt:Sn atomic ratios.

The cyclic voltammetry experiments were done at a scan rate of 10 mV s^{-1} in 1.0 mol L^{-1} KOH solution (between -0.9 V and -0.2 V vs Ag/AgCl) or 0.5 mol L^{-1} H_2SO_4 (between 0.05 and 0.80 V vs hydrogen reference) in the absence of ethanol saturated with N_2 . For acid electrolyte it was utilized a hydrogen reference electrode, graphite as work electrode and a counter electrode of Pt wire, while in alkaline electrolyte it was used KOH solution, Ag/AgCl (3.0 mol L^{-1} KCl) as reference electrode and a counter electrode of Pt and graphite as work electrode.

Ethanol oxidation were performed by chronoamperometry experiments in an Autolab 302N potentiostat, at $25 \text{ }^\circ\text{C}$ in a 0.5 mol L^{-1} H_2SO_4 solution for acid electrolyte, while alkaline experiments were performed in 1.0 mol L^{-1} KOH solution, where the chronoamperometry was recorded in KOH electrolyte containing ethanol, at -0.35 V , for 1800 s while for acid media the experiment was conducted at 0.5 V , for 1800 s .

Direct alkaline or acidic ethanol fuel cells experiments were performed in a single cell with 5 cm^2 of area, where the polarization curves were obtained using an AutoLab PGSTAT302N Potentiostat connected in the fuel cell and a panel of cell experiments Electrocell[®] Group. The membrane electrodes assemblies (MEA) were prepared by hot pressing of a pretreated Nafion[®] 117 membrane placed between anode and cathode. PtSn/C- In_2O_3 . SnO_2 with different atomic ratios was utilized as anode with 1.0 mg of Pt loading by cm^2 , while the cathode electrode was constructed with Pt/C BASF (1 mg of Pt loading by cm^2). The polarization curves in acid electrolyte were obtained using ethanol 2.0 mol L^{-1} and it was delivered at 2.0 mL min^{-1} with oxygen flow regulated at 150 mL min^{-1} . The temperature was set to $80 \text{ }^\circ\text{C}$ for the fuel cell and $85 \text{ }^\circ\text{C}$ for the oxygen humidifier. The polarization curves in alkaline electrolyte were obtained using 6.0 mol L^{-1} KOH + 2.0 mol L^{-1} ethanol being the fuel delivered at 2.0 mL min^{-1} .

3. RESULTS AND DISCUSSION

Pt:Sn atomic ratios were obtained by EDX. The values obtained were much similar to the nominal atomic ratios used during synthesis. Thus, the mean crystallite sizes determined using Scherrer equation is in the range of $3.0 - 4.0 \text{ nm}$ (Table 1).

Table 1. Pt:Sn atomic ratios and mean particle size of the prepared electrocatalysts.

Electrocatalysts	Atomic ratio (nominal)	Atomic ratio (EDX)	Average crystallite size (nm)
PtSn/C	70:30	75:25	3.0
PtSn/C-ITO	90:10	89:11	4.0
PtSn/C-ITO	70:30	73:27	3.0
PtSn/C-ITO	50:50	59:41	3.0

The X-ray diffractograms of PtSn/C- In_2O_3 . SnO_2 electrocatalysts are shown in Figure 1. In all diffractograms, it was observed a broad peak at about 25° that can be associated with the Vulcan XC72

support and four peaks at approximately $2\theta = 40^\circ$, 47° , 67° and 82° , which are associated with the (111), (200), (220) and (311) planes, respectively, of the fcc structure characteristic of platinum and platinum alloys.

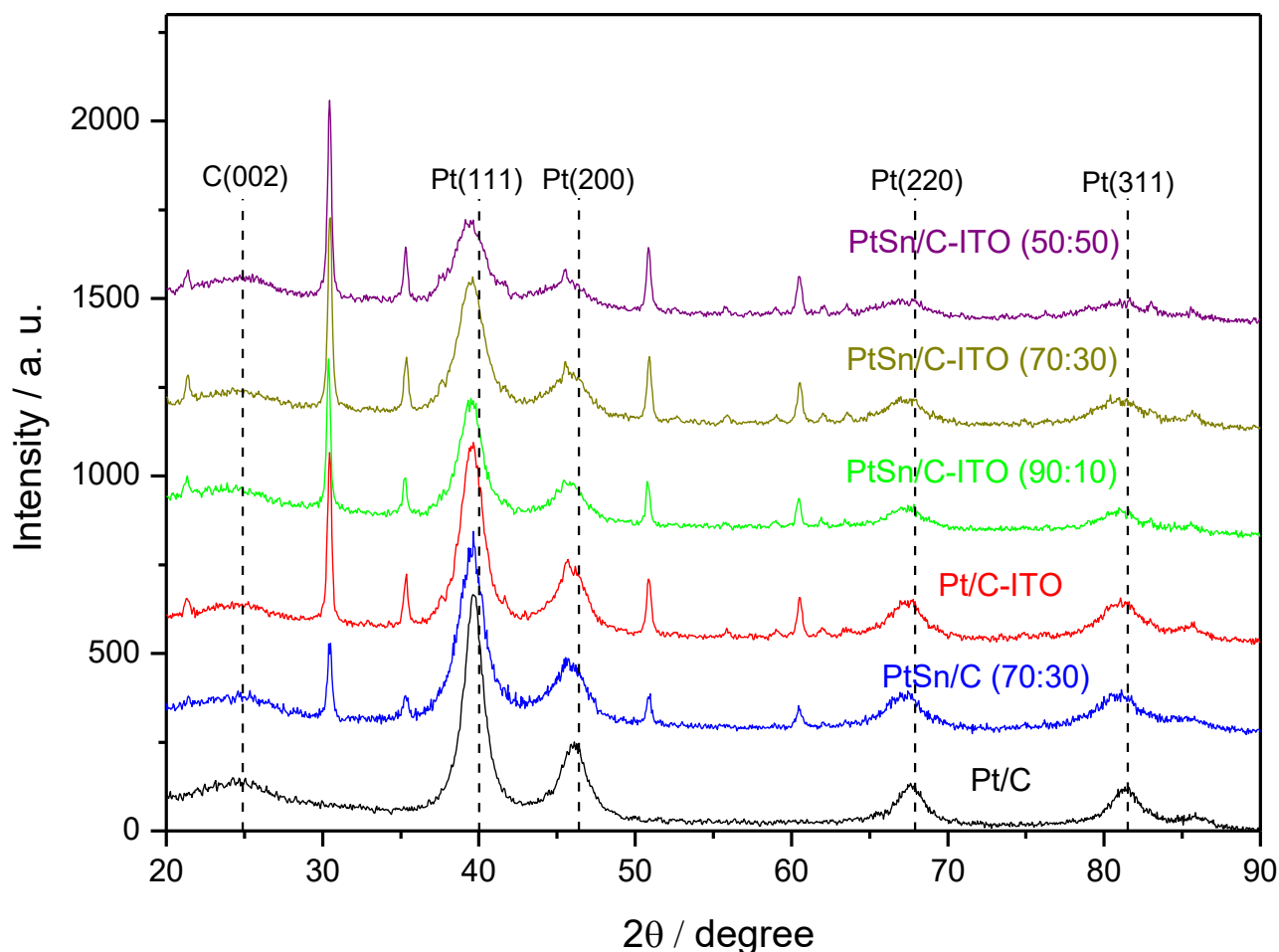


Figure 1. X-ray diffractograms of the Pt/C, Pt/C-ITO PtSn/C (70:30), PtSn/C-ITO (90:10), PtSn/C-ITO (70:30) and PtSn/C-ITO (50:50).

For PtSn/C- $\text{In}_2\text{O}_3\cdot\text{SnO}_2$ electrocatalysts it was also observed peaks at about $2\theta = 31^\circ$, 36° , 51° , 60° correspond to the (222), (400), (440) and (622) planes characteristic of In_2O_3 cubic structure. This result is in accordance with the works of Parrondo et al [12] and Henrique [11]. For PtSn/C and PtSn/C- $\text{In}_2\text{O}_3\cdot\text{SnO}_2$ electrocatalysts, shifts to 2θ values were observed compared with Pt/C patterns. This effect could be associated to the inclusion of Sn atoms to the fcc structure of Pt. The lattice parameters values for Pt/C, PtSn/C (70:30), PtSn/C- $\text{In}_2\text{O}_3\cdot\text{SnO}_2$ (90:10), PtSn/C- $\text{In}_2\text{O}_3\cdot\text{SnO}_2$ (70:30) and PtSn/C- $\text{In}_2\text{O}_3\cdot\text{SnO}_2$ (50:50) were 0.3917nm, 0.3924 nm, 0.3917 nm, 0.3929nm and 0.3955 nm, respectively. These results indicating that Sn atoms are added to Pt fcc structure.

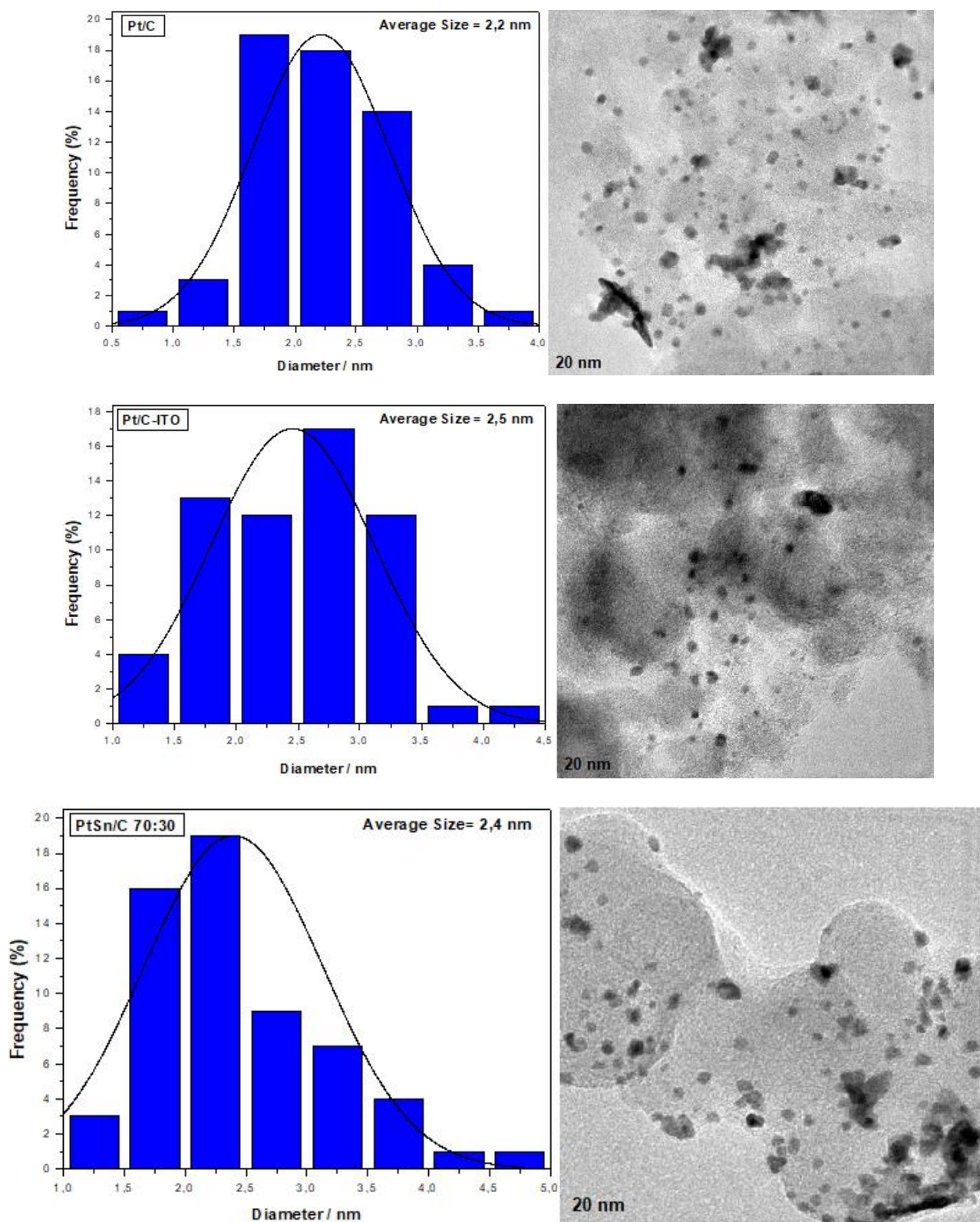


Figure 2a. TEM images and histograms of the particle size distribution to Pt/C, Pt/C-ITO and PtSn/C (70:30) electrocatalysts.

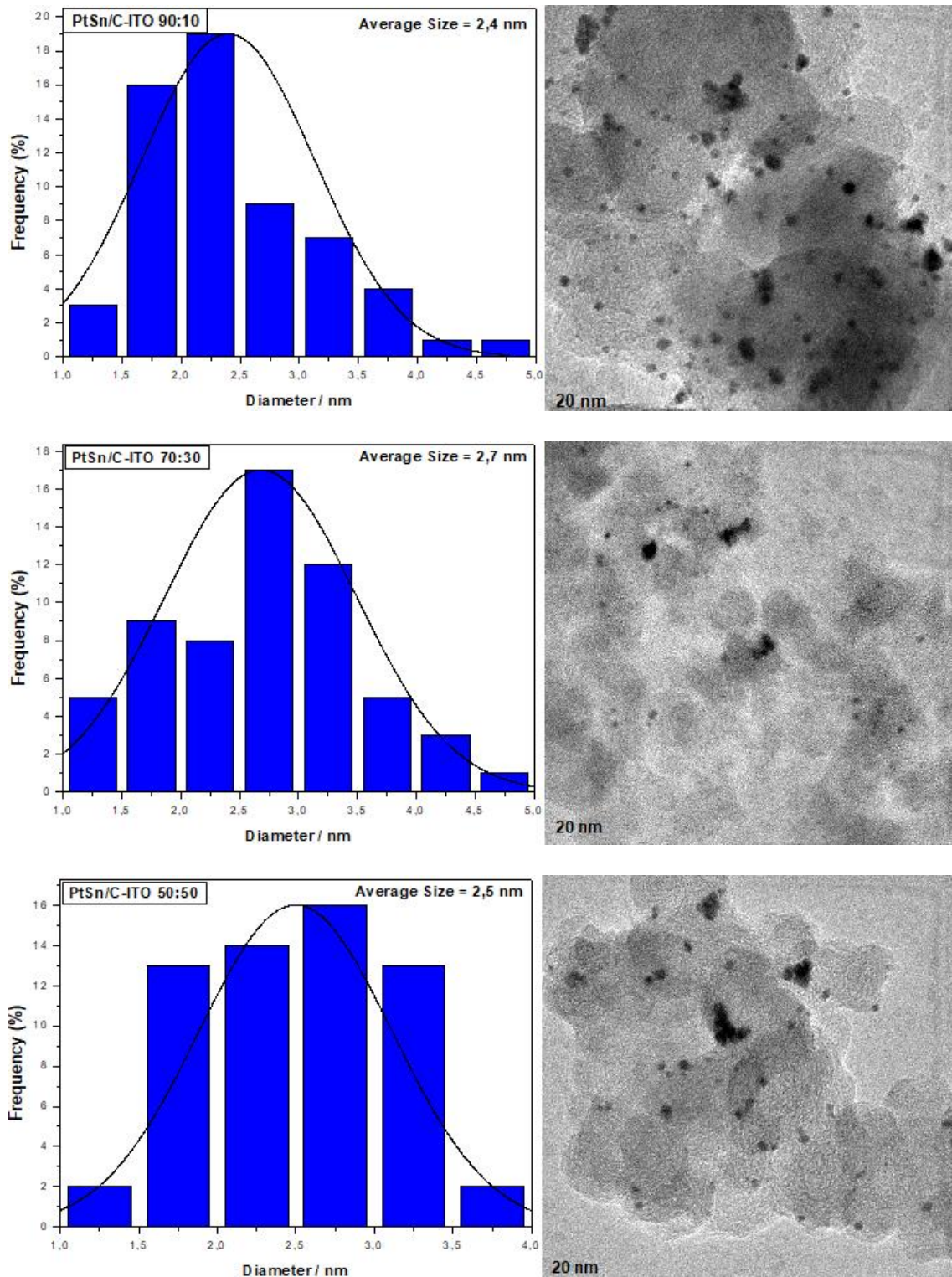


Figure 2b. TEM images and histograms of the particle size distribution to PtSn/C-ITO (90:10), PtSn/C-ITO (70:30) and PtSn/C-ITO (50:50) electrocatalysts.

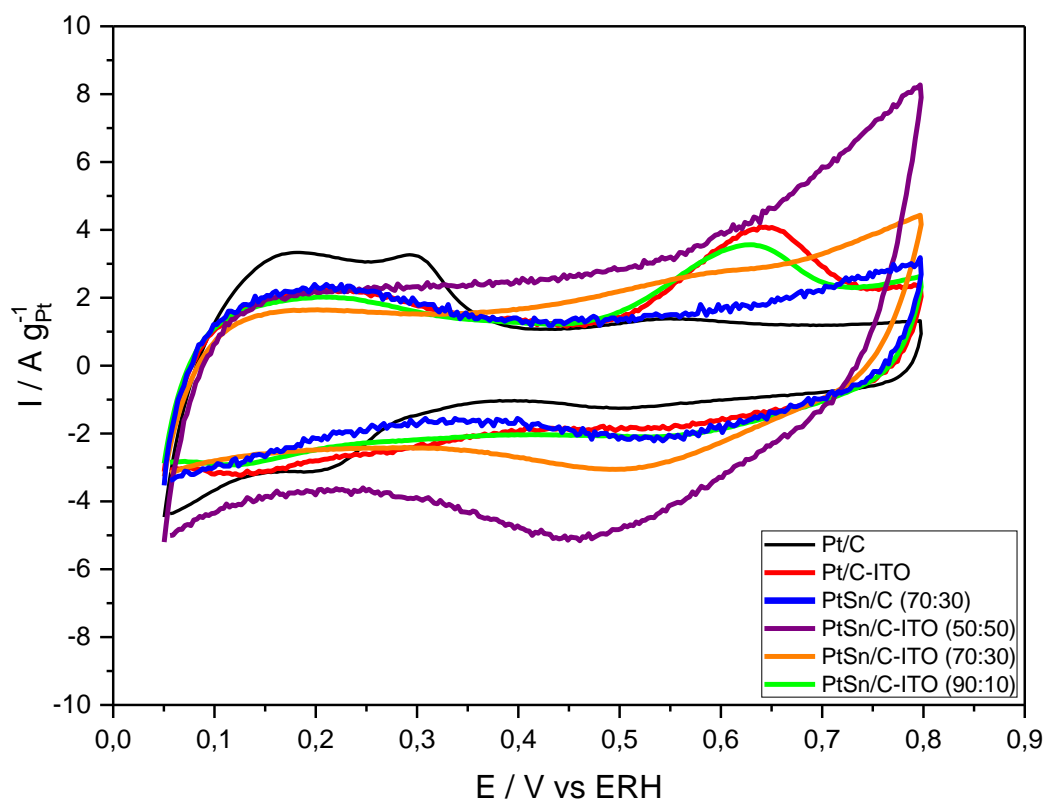
The micrographs and histograms of the nanoparticle size distribution of Pt/C, Pt/C- $\text{In}_2\text{O}_3\cdot\text{SnO}_2$, PtSn/C (70:30), PtSn/C- $\text{In}_2\text{O}_3\cdot\text{SnO}_2$ (90:10), PtSn/C- $\text{In}_2\text{O}_3\cdot\text{SnO}_2$ (70:30) and PtSn/C- $\text{In}_2\text{O}_3\cdot\text{SnO}_2$ (50:50) obtained by TEM are illustrated in Figures 2a and 2b. The mean diameter of the nanoparticles for Pt/C, Pt/C- $\text{In}_2\text{O}_3\cdot\text{SnO}_2$, PtSn/C (70:30), PtSn/C- $\text{In}_2\text{O}_3\cdot\text{SnO}_2$ (90:10), PtSn/C- $\text{In}_2\text{O}_3\cdot\text{SnO}_2$ (70:30)

and PtSn/C-In₂O₃.SnO₂ (50:50) were 2.2 nm, 2.5 nm, 2.4nm, 2.4 nm, 2.7 nm and 2.5 nm, respectively. Moreover all electrocatalysts prepared showed a good distribution of the nanoparticles on the support and some agglomerates, lastly the morphologies were not significantly changed. These results were similar to the work of Henrique et al. [11], where Pt/C electrocatalysts and Pt/C-In₂O₃.SnO₂ electrocatalyst showed particles with average sizes of 3.0 nm. In another work Ayoub et al. [10] showed a PtSn/C (50:50) prepared by an alcohol-reduction process with the mean particles sizes of 2.2 nm.

Cyclic voltammograms in absence of ethanol for Pt/C, Pt/C- In₂O₃.SnO₂, PtSn/C (70:30), PtSn/C-In₂O₃.SnO₂ (90:10), PtSn/C-In₂O₃.SnO₂ (70:30) and PtSn/C-In₂O₃.SnO₂ (50:50) in acidic and alkaline electrolytes are shown in Figure 3.

Fig. 3 display the typical profile of the hydrogen absorption/desorption on carbon supported PtSn, where Pt/C electrocatalyst shows a hydrogen adsorption/desorption area (0.05 - 0.40 V) higher than PtSn/C and all PtSn/C-In₂O₃.SnO₂.

It has been reported in the literature that the Sn presence inhibits these characteristic peaks, for blocking the active hydrogen-adsorption sites on the surface of Pt through geometric effects and for modifying electronic properties [3].



(A)

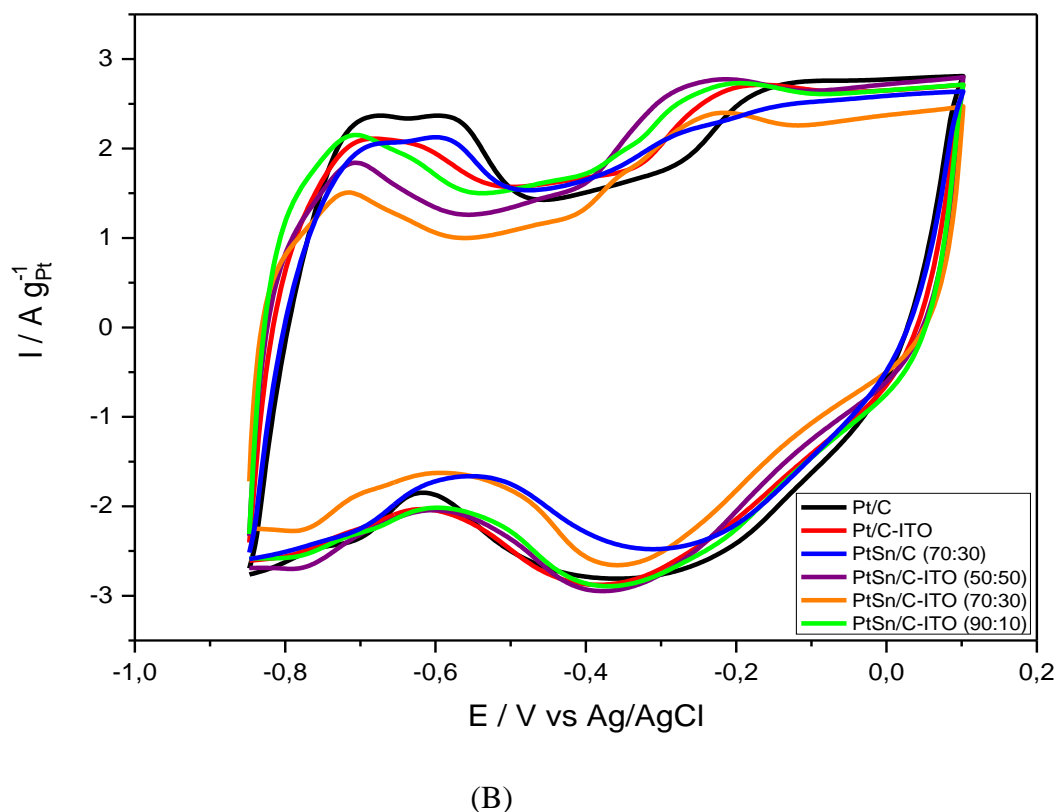


Figure 3. Cyclic voltammograms of Pt/C, Pt/C- $\text{In}_2\text{O}_3\cdot\text{SnO}_2$, PtSn/C (70:30), PtSn/C- $\text{In}_2\text{O}_3\cdot\text{SnO}_2$ (90:10), PtSn/C- $\text{In}_2\text{O}_3\cdot\text{SnO}_2$ (70:30) and PtSn/C- $\text{In}_2\text{O}_3\cdot\text{SnO}_2$ (50:50) electrocatalysts in (A) $0.5 \text{ mol L}^{-1} \text{ H}_2\text{SO}_4$ and (B) $1 \text{ mol L}^{-1} \text{ KOH}$ solution with a scan rate of 10 mV s^{-1} at 25°C .

The cyclic voltammograms in acidic electrolyte showed an increase in the currents in the double layer ($0.4\text{--}0.8 \text{ V}$), what can be attributed to the tin oxide species; this effect was more pronounced with an increasing amount of tin in PtSn electrocatalysts, as capacitance and resistance that also could influence in current values at double layer region. Pt/C- $\text{In}_2\text{O}_3\cdot\text{SnO}_2$ electrocatalyst shows an increase in the current values in the double layer ($0.4 - 0.8 \text{ V}$) in comparison with Pt/C, this effect can be attributed to the contribution of Pt and ITO oxide species [16], where the anodic peaks appeared around 0.6V indicates the oxidation of In-O species [12]. Pt/C- $\text{In}_2\text{O}_3\cdot\text{SnO}_2$ electrocatalyst did not show a well-defined hydrogen adsorption–desorption region ($0.05\text{--}0.4 \text{ V}$) in comparison with Pt/C electrocatalysts, this effect can be also attributed to the presence or the oxidation of In-O species [11].

Pt/C- $\text{In}_2\text{O}_3\cdot\text{SnO}_2$, PtSn/C and all PtSn/C- $\text{In}_2\text{O}_3\cdot\text{SnO}_2$ did not show a well-defined hydrogen oxidation region (-0.85 to -0.60 V versus Ag/AgCl $3.0 \text{ mol L}^{-1} \text{ KCL}$) in comparison to pure platinum, because the Sn presence inhibits these characteristic peaks. Finally, the current densities in the double layer region of Pt/C- $\text{In}_2\text{O}_3\cdot\text{SnO}_2$, PtSn/C and all PtSn/C- $\text{In}_2\text{O}_3\cdot\text{SnO}_2$ were similar than those obtained with Pt/C, this result was different to what was observed in acidic electrolyte; indicating that the formation of tin oxides species was not favored in alkaline electrolyte in comparison with acid electrolyte studies.

Chronoamperometry results for Pt/C, Pt/C-In₂O₃.SnO₂, PtSn/C (70:30), PtSn/C-In₂O₃.SnO₂ (90:10), PtSn/C-In₂O₃.SnO₂ (70:30) and PtSn/C-In₂O₃.SnO₂ (50:50) in presence of 0.5 mol L⁻¹ H₂SO₄ + 1.0 mol L⁻¹ ethanol in range potential of 0.5 V, for 30 min or 1.0 mol L⁻¹ KOH + 1 mol L⁻¹ ethanol in -0.35 V, for 30 min, are illustrated in Figure 4.

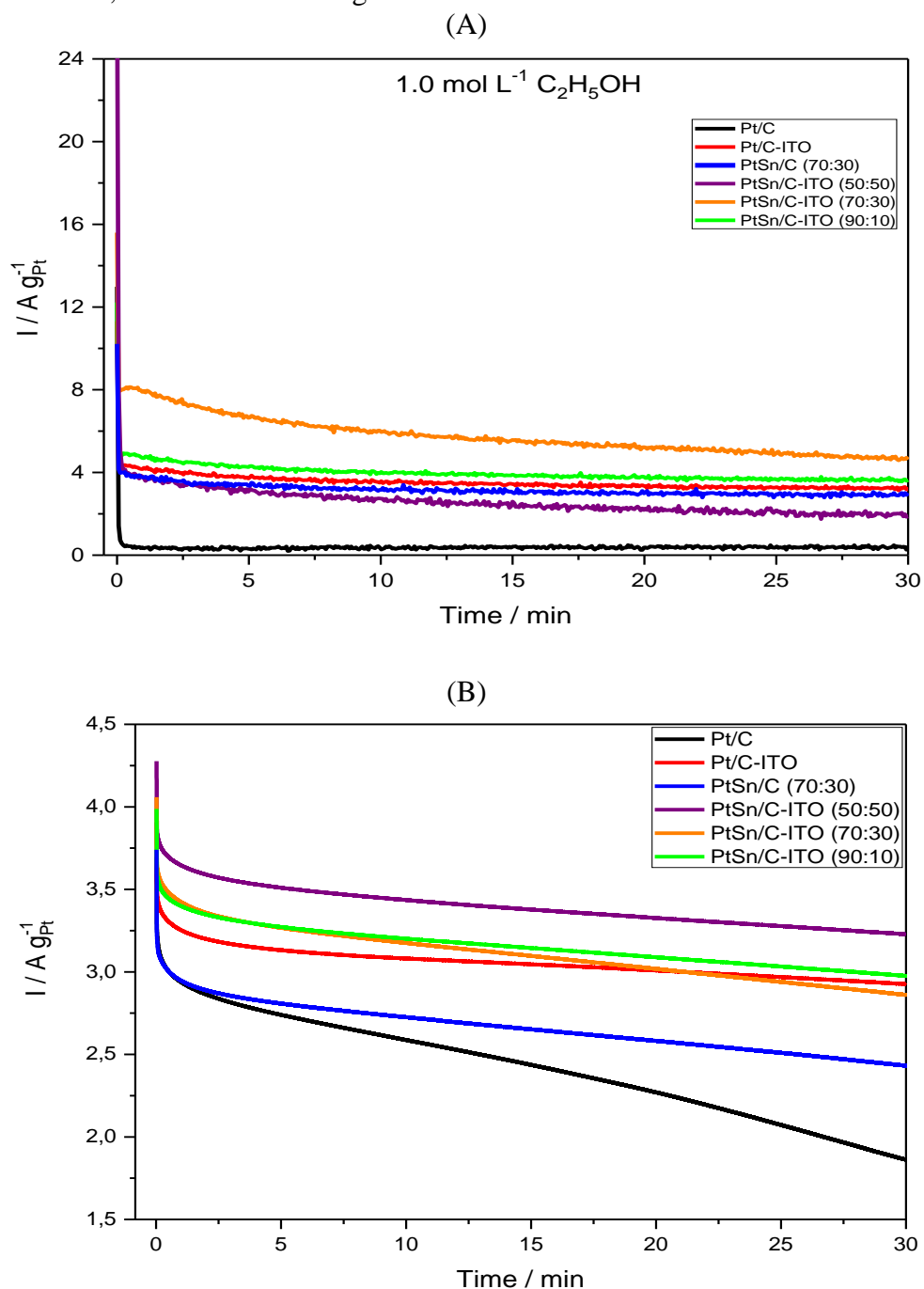
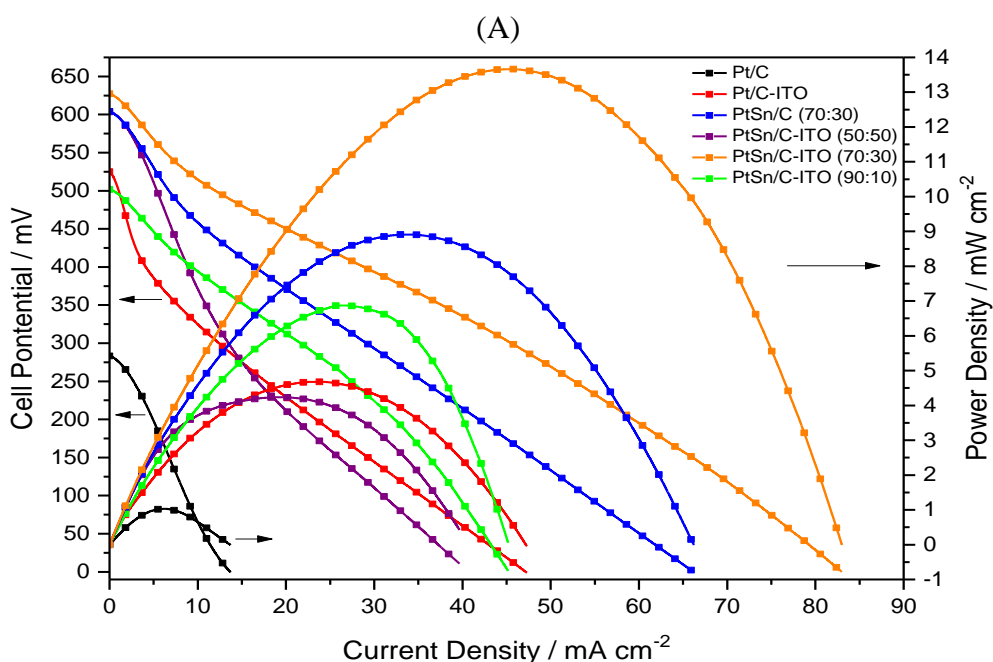


Figure 4. Chronoamperometry curves in presence of 0.5 mol L⁻¹ H₂SO₄ + 1.0 mol L⁻¹ ethanol at 0.5 V by 30 minutes (A) or 1 mol L⁻¹ KOH + 1 mol L⁻¹ ethanol at -0.35 V by 30 minutes (B) for Pt/C, Pt/C-In₂O₃.SnO₂, PtSn/C (70:30), PtSn/C-In₂O₃.SnO₂ (90:10), PtSn/C-In₂O₃.SnO₂ (70:30) and PtSn/C-In₂O₃.SnO₂ (50:50) electrocatalysts.

The current–time curves in acidic electrolyte for all PtSn/C-In₂O₃.SnO₂ and PtSn/C (70:30) showed higher current densities than Pt/C. This was observed in following order of activity: PtSn/C-In₂O₃.SnO₂ (70:30) > PtSn/C-In₂O₃.SnO₂ (90:10) > Pt/C-In₂O₃.SnO₂ > PtSn/C (70:30) > PtSn/C-In₂O₃.SnO₂ (50:50) > Pt/C. These results prove the beneficial effect the addition of Sn and In₂O₃.SnO₂ to Pt, what could be explained by the oxy-hydroxy interactions that occur in the catalytic layer and to electronic effect associated with the formation of PtSn alloy. Furthermore, according to Shuaiba et al [13] the good interaction between SnO₂ and Pt could prevent agglomerations, provide high surface area and also high CO tolerance, explaining. The obtained results showed an optimization of 30% tin in the composition of the PtSn/C-In₂O₃.SnO₂ electrocatalyst.

For alkaline electrolyte it was observed the following order of activity: PtSn/C-In₂O₃.SnO₂ (50:50) > PtSn/C-In₂O₃.SnO₂ (90:10) > Pt/C-In₂O₃.SnO₂ > PtSn/C-In₂O₃.SnO₂ (70:30) > PtSn/C (70:30) > Pt/C. In alkaline electrolyte was observed for all electrocatalysts a great initial current drop; that is associated to a rapid increase of the surface coverage by partially oxidized species that block Pt surfaces, diminishing its ability to electro-oxidize ethanol [9].

Figure 5 shows the performances of (a) direct ethanol fuel cell and (b) direct alkaline methanol fuel cell with Pt/C, Pt/C-In₂O₃.SnO₂, PtSn/C (70:30), PtSn/C-In₂O₃.SnO₂ (90:10), PtSn/C-In₂O₃.SnO₂ (70:30) and PtSn/C-In₂O₃.SnO₂ (50:50), PtSn/C-In₂O₃.SnO₂ (70:30) was more active that Pt/C, Pt/C-In₂O₃.SnO₂ and others PtSn/C-In₂O₃.SnO₂ prepared by sodium borohydride reduction process in direct ethanol fuel cell.



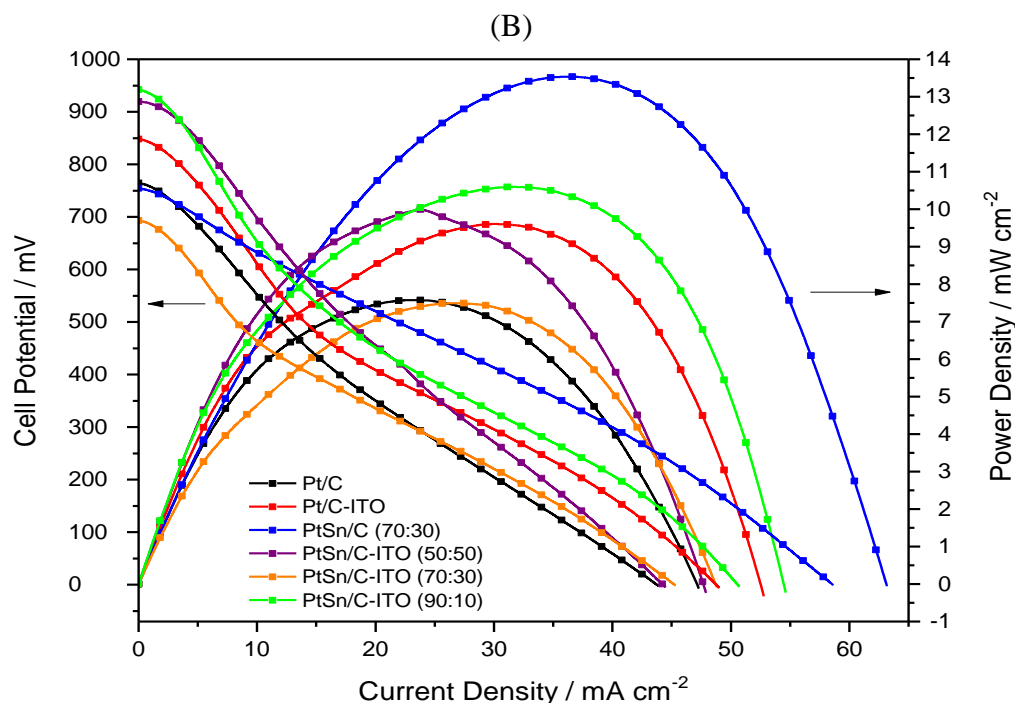


Figure 5. (A) Polarization curves and power density curves in a 5 cm² DMFC at 80 °C using Pt/C, Pt/C-In₂O₃.SnO₂, PtSn/C (70:30), PtSn/C-In₂O₃.SnO₂ (90:10), PtSn/C-In₂O₃.SnO₂ (70:30) and PtSn/C-In₂O₃.SnO₂ (50:50) electrocatalysts as anode catalysts (1 mg Pt cm⁻²) and Pt/C BASF as the cathode catalyst (1 mg Pt cm⁻²), Nafion® 117 was used as the membrane ethanol 2 mol L⁻¹ with 2.0 mL min⁻¹ flux and oxygen pressure (2 bar). (B) I-V polarization curves and the power density curves at 80 °C of a 5 cm² DAMFC using Pt/C, Pt/C-In₂O₃.SnO₂, PtSn/C (70:30), PtSn/C-In₂O₃.SnO₂ (90:10), PtSn/C-In₂O₃.SnO₂ (70:30) and PtSn/C-In₂O₃.SnO₂ (50:50) electrocatalysts electrocatalysts as anodes (1 mg Pt cm⁻² catalyst loading) and Pt/C BASF electrocatalyst cathode (1 mg Pt cm⁻² catalyst loading with 20 wt% Pt loading on carbon), Nafion® 117 membrane treated with KOH, 1.0 mol L⁻¹ KOH + 2.0 mol L⁻¹ ethanol was using as fuel.

These results are agreement with chronoamperometry results. All PtSn/C-In₂O₃.SnO₂ also were more activity in comparison with Pt/C and Pt/C-In₂O₃.SnO₂ confirming the beneficial effect of tin addition to Pt. Pt/C-In₂O₃.SnO₂ also was more activity than Pt/C, where this effect may be due to the synergistic interaction between Pt and In₂O₃ and the surface effect of the nanoparticles In₂O₃ [17]. The In₂O₃ oxides also could have active sites for the formation of oxygen-containing species, which will help to oxidize the adsorbed intermediate species according to the bifunctional mechanism.

The open circuit voltage of the alkaline direct ethanol alkaline fuel cell containing PtSn/C (70:30) was 0.754V, while the corresponding value for Pt/C was approximately 0.764 V. These results showed that not always higher values of the open circuit voltage influence on the performance of power density of the electrocatalysts, therefore, the PtSn/C (70:30) indicated the highest value of maximum power density with relation to others electrocatalysts prepared, probably due to the synergism among the constituents of the electrocatalysts (metallic Pt and Sn). The formation of chemisorbed oxygenated species that promotes the oxidation of adsorbed carbon monoxide or adsorbed intermediate on the surface of platinum should be considered. These results are in disagreement with

chronoamperometry results, probably because of the low conductivity of Nafion membrane material. Finally the development of new anionic membranes and alkaline ionomer are strongly encouraged for better results in DAEFC [18].

4. CONCLUSIONS

The method utilized in this work was an efficient process to produce PtSn/C-In₂O₃.SnO₂ for ethanol oxidation in alkaline and acidic electrolytes. PtSn/C-In₂O₃.SnO₂ electrocatalysts showed peaks associated the face-centered cubic (fcc) structure of platinum, peaks which could be identified as a cassiterite SnO₂ phase or with Indium-doped SnO₂ (ITO) used as supports. All PtSn/C-In₂O₃.SnO₂ showed a shift to higher 2θ values in comparison with Pt/C electrocatalysts; this effect could be associated to the formation of PtSn alloys.

PtSn/C-In₂O₃.SnO₂ exhibited superior performance for ethanol oxidation (chronoamperometry) in both electrolytes in comparison with Pt/C and PtSn/C, where the high values of currents for these electrocatalysts could be related to the combination of the bifunctional mechanism and the electronic effect or to the synergetic interaction between PtSn and In₂O₃.

Experiments in Direct methanol fuel cells showed that the power density values obtained for PtSn/C-In₂O₃.SnO₂ (70:30) and PtSn/C (70:30) was higher than Pt/C for acid and alkaline studies, respectively. These results are in disagreement with chronoamperometry and an explanation could be associated to the low conductivity of Nafion membrane material for alkaline studies, therefore the development of new anionic membranes and alkaline ionomer should be strongly encouraged by the promising results from direct alkaline fuel cell experiments.

Finally, further research is necessary to investigate the mechanisms of ethanol oxidation in alkaline and acidic electrolytes using PtSn/C-In₂O₃.SnO₂ electrocatalysts and to investigate the surface of these materials through XPS analysis.

ACKNOWLEDGEMENTS

The authors thank the Laboratório de Microscopia do Centro de Ciências e Tecnologia de Materiais (CCTM) by TEM measurements and FAPESP (2014/09087-4, 2014/50279-4) and CNPQ (300816/2016-2) for the financial support.

References

1. P.J.S. Maia, E.M. Barboza, M.L. Veja, H.N. da Cunha, E.A. de Souza and F.A. de Freitas, *Chem. Papers*, 72 (2018) 1021.
2. N.S. Veizaga, V.A. Paganin, T.A. Rocha, O.A. Scelza, S.R. de Miguel and E.R. Gonzalez, *Int. J. hydrogen energy*, 39 (2014) 8728.
3. P.G. Corradini and J. Perez, *J. Solid State Electrochem.*, 22 (2018) 1525.
4. D.R.M. Godoi, J. Perez and H.M. Villullas, *J. Power Sources*, 195 (2010) 3394.
5. X. Fang, L.Q. Wang, P.K. Shen, G.F. Cui and C. Bianchin, *J. Power Sources*, 195 (2010) 1375.
6. F. Vigier, C. Coutanceau, A. Perrard, E.M. Belgsir and C. Lamy, *J. Appl. Electrochem.*, 34 (2004) 439.

7. R.G. Freitas, L.F.Q.P. Marchesi, M.R. Forim, L.O.S. Bulhões, E.C. Pereira, M.C. Santos and R.T.S. Oliveira, *J. Braz. Chem. Soc.*, 22 (2011) 1709.
8. J.M. Sieben and M.M.E. Duarte, *Int. J. Hydrogen Energy*, 36 (2011) 3313.
9. E.A. Baranova, M.A. Padilha, B. Hallevi, T. Amir, K. Artyushkova and P. Atanassov, *Electrochim. Acta*, 80 (2012) 377.
10. J.M.S. Ayoub, R.F.B. de Souza, J.C.M. Silva, R.M. Piasentin, E.V. Spinacé, M.C. Santos and A.O. Neto, *Int. J. Electrochem. Sci.*, 7 (2012) 11351.
11. R.S. Henrique, R.F.B. de Souza, J.C.M. Silva, J.M.S. Ayoub, R.M. Piasentin, M. Linardi, E.V. Spinacé, M.C. Santos and A.O. Neto, *Int. J. Electrochem. Sci.*, 7 (2012) 2036.
12. J. Parrondo, R. Santhanam, F. Mijangos and B. Rambabu, *Int. J. Electrochem. Sci.*, 5 (2010) 1342.
13. S. Shuaiba, L. Kee Shyuan, W. Wai Yin, L. Tian Khoon, S. Jaka, C. Seng Tong and D. Wan Ramli Wan, *Int. J. hydrogen energy*, 43 (2018) 7823.
14. S. Park, Y. Shao, V.V. Viswanathan, J. Liu and Y. Wang, *J. Ind. Eng. Chem.*, 42 (2016) 81.
15. F. Colmati, E. Antolini and E.R. Gonzalez, *J. Electrochem. Soc.*, 154 (2007) B39.
16. R.M.S. Rodrigues, R.R. Dias, C.A.L.G.O. Forbicini, M. Linardi, E.V. Spinacé and A.O. Neto, *Int. J. Electrochem. Sci.*, 6 (2011) 5759.
17. D. Chu, J. Wang, L. Zha, J. He, H. You, Y. Yan, H. Lin and Z. Tian, *Catal. Communications*, 10 (2009) 955.
18. A. Santasalo-Aarnio, S. Tuomi, K. Jalkanen, K. Kontturi and T. Kallio, *Electrochim. Acta*, 87 (2013) 730.